Clinical Imaging 57 (2019) 7–14

Contents lists available at ScienceDirect

Clinical Imaging

journal homepage: www.elsevier.com/locate/clinimag

Cardiothoracic Imaging

Coronary plaque composition assessed by cardiac computed tomography using adaptive Hounsfield unit thresholds

Martina Chantal de Knegt[a,*], Morten Haugen[a], Andreas Kryger Jensen[b], Jesper James Linde[a], Jørgen Tobias Kühl[a], Jens Dahlgaard Hove[c], Klaus Fuglsang Kofoed[a,d]

[a] Department of Cardiology, Rigshospitalet, University of Copenhagen, Copenhagen, Denmark
[b] Biostatistics, Institute of Public Health, University of Copenhagen, Copenhagen, Denmark
[c] Department of Cardiology, Hvidovre Hospital, University of Copenhagen, Copenhagen, Denmark
[d] Department of Radiology, Rigshospitalet, University of Copenhagen, Copenhagen, Denmark

ARTICLE INFO

Keywords:
Cardiac computed tomography
Plaque characterization
Plaque composition
Coronary atherosclerosis
Coronary artery disease

ABSTRACT

Purpose: Quantitative computed tomography (QCT) may be useful in detecting high-risk patients with coronary atherosclerosis. Assessment of plaque composition using fixed Hounsfield unit (HU) thresholds is influenced by luminal contrast density. A method using adaptive HU thresholds has therefore been developed. This study investigates agreement between plaque volumes derived using fixed and adaptive HU thresholds and the influence of luminal contrast density on the determination of plaque composition.

Methods: We performed QCT in 260 patients with recent acute-onset chest pain without acute coronary syndrome. Plaque volumes of necrotic core (NC), fibrous fatty (FF), fibrous (FI) and dense calcium (DC) tissue were measured in 1161 coronary segments. Agreement between plaque volumes using fixed and adaptive HU thresholds was tested using the Bland-Altman method. Additionally, patients were stratified into tertiles of ascending aortic luminal contrast density and plaque volumes were compared.

Results: Bland-Altman plots revealed that fixed HU thresholds underestimated FI and FF plaque volumes and overestimated NC and DC plaque volumes compared to adaptive HU thresholds. Volumes of dense calcium plaque differed with increasing tertiles of luminal contrast density when using fixed HU thresholds but not when using adaptive HU thresholds: DC for fixed HU thresholds (mm^3, median (95%CI)): 7.73 (5.17;12.31), 9.83 (6.55;13.57), 12.02 (8.26;16.24); DC for adaptive HU thresholds (mm^3, median (95%CI)): 7.34 (5.12;12.03), 7.78 (5.40;12.61), 8.56 (5.22;12.69).

Conclusions: Plaque volumes by fixed and adaptive HU thresholds differed. Plaque volumes by adaptive HU thresholds were more independent of luminal contrast density for higher attenuation tissues compared to fixed HU thresholds.

1. Introduction

Coronary plaque composition is a key determinant of plaque stability and has been found to carry important prognostic information [1–5]. As such, plaque composition is being incorporated into coronary computed tomography angiography (CCTA) assessment recommendations and reliable determination of coronary plaque composition is therefore of paramount importance [6]. New semi-automated quantitative techniques for the assessment of plaque composition have emerged and have shown good intra and interobserver reproducibility [7,8]. Quantitative computed tomography (QCT) could therefore, in the future, supplement conventional CCTA reading as an effective, accurate and user-independent technique.

The most predominant method of determining plaque composition using QCT is to use predefined fixed thresholds on the Hounsfield unit (HU) scale to differentiate between different tissue types. It has been shown, however, that luminal contrast density affects plaque tissue characterization [9,10]. Luminal contrast density is affected by a

Abbreviations: BMI, body mass index; BSA, body surface area; CAD, coronary artery disease; CATCH, Cardiac CT in the Treatment of Acute Chest Pain study; CCTA, coronary computed tomography angiography; DC, dense calcium; FF, fibrous fatty; FI, fibrous; HU, Hounsfield unit; IQR, interquartile range; IVUS VH, intravascular ultrasound virtual histology; NC, necrotic core (NC); NCP, non-calcified plaque; QCT, Quantitative computed tomography

* Corresponding author at: Department of Cardiology, The Heart Center, Rigshospitalet, Blegdamsvej 9, 2100 Copenhagen, Denmark.
E-mail addresses: martinadeknegt@gmail.com (M.C. de Knegt), aeje@sund.ku.dk (A.K. Jensen), jhove@dadlnet.dk (J.D. Hove), kkofoed@dadlnet.dk (K.F. Kofoed).

https://doi.org/10.1016/j.clinimag.2019.04.014
Received 22 July 2018; Received in revised form 8 April 2019; Accepted 24 April 2019

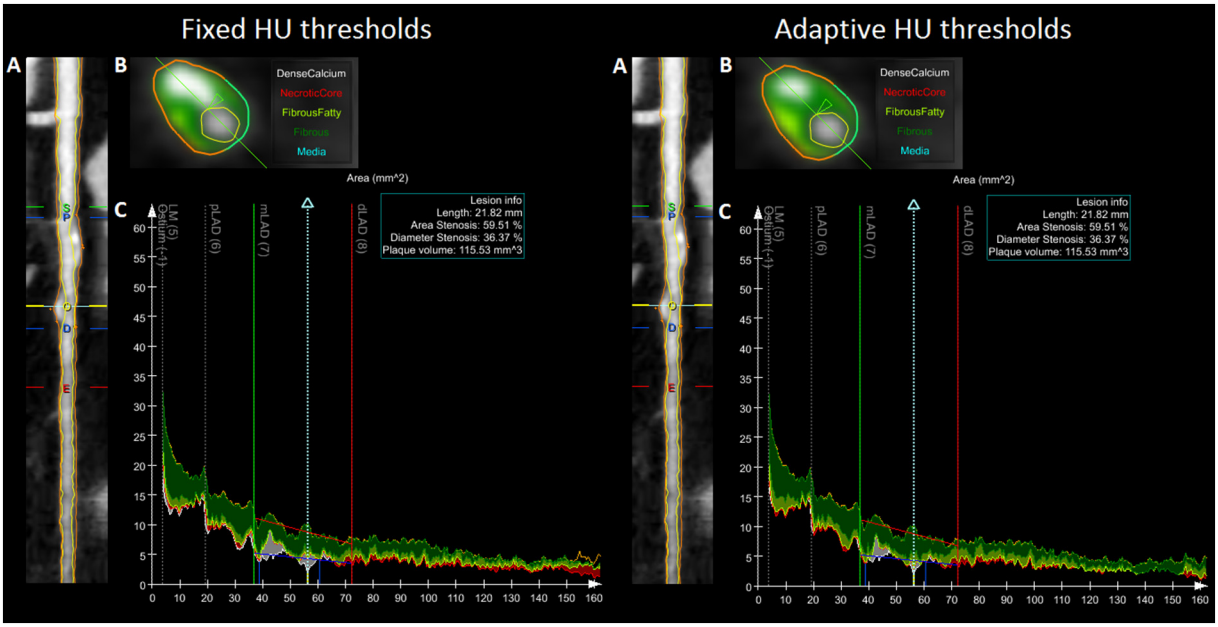

Fig. 1. Example of quantitative analysis of a mid-left anterior descending artery segment using fixed and adaptive Hounsfield unit thresholds. A) Longitudinal straightened multiplanar reconstruction where *S* and *E* are the start and end of the segment, respectively; *P* and *D* are the proximal and distal borders of the lesion, respectively; and *O* is the point of maximal obstruction. B) Transverse vessel view at the point of maximal obstruction with color overlay to illustrate plaque tissue types. From visual assessment of the color overlay, it can be seen that the fixed method characterizes this plaque as containing more dense calcium and less fibrofatty tissue compared to the adaptive method. C) Coronary plaque area-vessel length graph with color overlay to illustrate plaque tissue types.

variety of factors including patient body size and cardiac output [11] and, despite efforts to personalize scan protocols, it is well known that there is a large variability regarding density of the contrast bolus arriving to the coronary arteries. Furthermore, luminal contrast density has been found to decrease along the length of a vessel and is lower in vessel segments with severe stenosis [12,13]. To remedy these multiple issues, a novel method for assessment of plaque composition has been established which uses adaptive HU threshold values depending on regional attenuation of contrast in the lumen [12,13].

In a low risk unstable angina pectoris population, we aimed to investigate agreement between plaque volumes derived using fixed and adaptive HU thresholds and to examine the influence of luminal contrast density on the determination of plaque composition when using these two methods. Specifically, we hypothesize that 1) plaque tissue volumes by the adaptive and fixed methods differ and 2) the adaptive method adjusts for luminal contrast density and therefore measures plaque volumes more independently of luminal contrast density compared to fixed HU thresholds.

2. Material and methods

2.1. Design and study population

This study is a sub-study of the *Cardiac CT in the Treatment of Acute Chest Pain study*, (CATCH - clinical trial number NCT01534000) which included 600 patients presenting with acute chest pain in an emergency room setting without signs of acute coronary syndrome [14].

All participants were referred to CCTA at the Department of Cardiology and Radiology, Rigshospitalet, Copenhagen, Denmark. All patients gave written informed consent to have a CCTA performed and the local ethics committee approved individual study protocols. This study was approved by *The Danish Data Protection Agency* (j.nr. 2015-41-3805) and complies with the 2nd Declaration of Helsinki.

2.2. Coronary computed tomography angiography

CCTA was performed with a 320 multidetector scanner (Aquilion One, Vision Edition, Canon, Tokyo, Japan). Oral beta blockers (metoprolol) were given to all patients with a heart rate > 60 beats per minute if systolic blood pressure was > 100 mmHg and there were no other contraindications to beta blockade. If necessary, i.v. beta blocker (metoprolol) was given just before scanning. Overall scan protocol: 320 × 0.5 mm detector collimation, median (min-max) tube voltage 120 kV (100–135 kV) depending on body mass index (BMI), 500 (140–580) mA tube current, and 0.35–0.45 s gantry rotation time (heart rate dependent). Intravenous contrast media Omnipaque, GE Healthcare, Chalfont St. Giles, United Kingdom 350 mgI/mL was infused with a flow rate of 6.0 ml/s with a biphasic injection protocol followed by a saline chaser. Patients 60–100 kg received 70 ml of contrast and patients > 100 kg received 90 ml of contrast. The automatic bolus triggering technique with a region of interest placed in the descending aorta and 300 HU was used for initiating image acquisition. Reconstructions at best phase of the R-R interval using an automatic raw data motion analysis tool (PhaseXact, Toshiba) were performed. Images were reconstructed with 0.5 mm slice thickness and increments of 0.25 mm using filtered back projection and filter FC 03. The conversion factor 0.014 mSv / (mGy × cm) was used to calculate the estimated radiation dose.

2.3. Image analysis

Image analysis was performed by a single certified reader with two years of intensive reading experience. Patients without a contrast-enhanced CCTA and without coronary artery disease (CAD), assessed visually as the absence of any coronary atherosclerosis by CCTA, were excluded from this study. CCTA image quality was evaluated as poor, moderate or good by visual assessment. CCTA studies with poor image quality deemed unsuitable for semi-automated coronary plaque quantification due to motion, image noise, severe calcification, poor contrast timing, pacemaker artifacts, and field of view issues, were excluded, as described by Kühl et al. [15].

2.4. Plaque composition analysis

Quantitative analysis was performed using semi-automated quantitative analysis software (QAngioCT Research Edition version 2.1.9.1, Medis Medical Imaging Systems, Leiden, The Netherlands) [13,16], see Fig. 1. Firstly, vessel tracking was used to extract the coronary tree and generate straightened and curved multiplanar reformatted volumes [17]. Secondly, the lumen and vessel borders were delineated automatically and edited manually if necessary in both longitudinal and transverse vessel views [17]. Thirdly, segment borders in each coronary artery were determined according to *Society of Cardiovascular Computed* Tomography guidelines [18]. If no vessels branches were present to indicate segments borders, vessel lengths were divided into thirds to provide proximal, mid and distal segments. Using the 17-segment model, in vessel segments with coronary plaque, the proximal and distal borders of the plaque were determined visually and plaque volumes were automatically calculated. Segments with motion, severe noise, severe calcification, vessel diameter < 1.5 mm, or total occlusions with limited retrograde contrast filling, field of view issues, and stented segments were not assessed.

2.5. Fixed and adaptive method for the determination of plaque composition

The semi-automated quantitative analysis software allows for the determination of plaque composition using fixed and adaptive thresholds on the HU scale and uses predefined cut-off values for determining volumes of necrotic core (NC), fibrous fatty (FF), fibrous (FI) and dense calcium (DC) in each plaque. All coronary plaques were measured using both fixed and adaptive methods. The fixed thresholds for determination of plaque composition were defined as follows: NC -30 to 75 HU, FF 76 to 130 HU, FI 131 to 350 HU and DC 351 to 2048 HU [13]. The adaptive thresholds for determination of plaque composition are automatically corrected for luminal contrast density, as previously described [12,13] and is based on the theory that the determination of plaque composition is affected by luminal contrast density and that contrast density falls along the length of the vessel [9]. Fig. 2 illustrates an example of semi-automated plaque quantification using fixed and adaptive thresholds. In short, the adaptive thresholds for determining plaque tissue types are automatically adapted to luminal contrast density and are defined using the mean lumen density: The threshold for NC is fixed at 75 HU for lumen densities above 275 HU and lowers when the estimated lumen density is below 275 HU. The threshold for FF is fixed at 150 HU for lumen densities above 350 HU and lowers when estimated lumen density is below 350 HU. The threshold for FI is fixed at 450 HU for lumen densities above 350 HU and lowers when estimated lumen density is below 350 HU. DC is all HU values above the FI limits [12]. In addition, the threshold for NC is automatically decreased in the presence of a severe stenosis due to the theory that severe stenosis results in decreased distal contrast density. Similarly, the threshold for DC is automatically increased in areas with calcified tissue as blooming artifacts increase lumen density and may also affect the determination of the composition of neighboring plaque.

2.6. Data analysis

Coronary plaque volumes measured using fixed and adaptive HU thresholds were compared at lesion level. Furthermore, luminal contrast density was measured in HU in the aorta (HU_{aorta}) just cranial of the ostia of the coronary arteries using an external workstation (Vitrea 2, version 6.7, Vital Images Inc., Plymouth, Minnesota). Patients were stratified into tertiles according to HU_{aorta} and plaque volumes determined using fixed and adaptive thresholds were compared at lesion level across these HU_{aorta} tertiles.

2.7. Statistics

Normal distributed variables are summarized as mean ± SD, otherwise as median and interquartile range (IQR). Categorical variables are summarized as frequencies and proportions. One-way analysis of variance and the Kruskal-Wallis test were used to assess differences in normal and non-normal distributed data, respectively. The χ^2-test was used to test for differences in categorical data. Agreement between

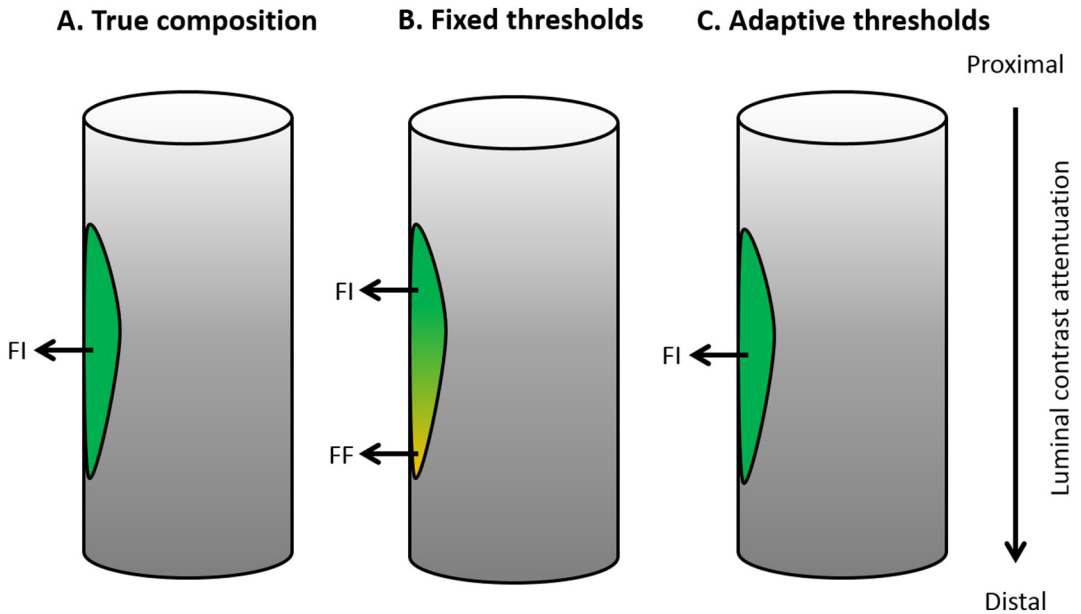

Fig. 2. Illustration of a semi-automated quantitative plaque measurement in a coronary vessel segment by CCTA. A. A theoretical depiction of true coronary plaque composition. B. Distally located regions of plaque are less influenced by lumen contrast density and therefore have lower attenuation than proximally located regions of plaque. In this example, distal regions of plaque are therefore incorrectly classified as FF when using fixed thresholds. C. Adaptive thresholds correct for luminal contrast density by reducing FI Hounsfield unit thresholds where luminal contrast density is low, i.e. in distal vessel regions. In this example, distal regions of plaque are therefore correctly classified as FI.
FI, Fibrous; FF, Fibrous fatty.

DC, FI, FF and NC plaque volumes derived using the fixed and adaptive methods was assessed by Bland-Altman plots showing differences between the two methods against their averages [19]. A spline regression model was used to estimate the expected relationship between differences and averages on the population level, and 2.5% and 97.5% probability intervals were estimated by non-parametric quantile regression [20] with a spline parameterization. Plaque volumes stratified by tertile of HU_{aorta} are given as medians and 95% confidence intervals calculated using a cluster level bootstrap with 25,000 replicate and the percentile method. The Wilcoxon rank-sum test adjusted for repeated measures on the subject level by the Datta-Satten method was used to compare plaque volumes across HU_{aorta} tertiles [21]. The Wilcoxon signed-rank test adjusted for clustering using the Rosner-Glynn-Lee method was used to compare plaque volumes using fixed and adaptive HU thresholds [22]. Statistical analyses were performed using IBM SPSS Statistics, version 22.0; Armonk, NY: IBM Corp, and R [23]. *P*-values below 5% were considered statistically significant.

3. Results

3.1. Study population

Among patients included in the CATCH trial, 59 subjects did not undergo a contrast-enhanced CCTA and 281 subjects who underwent CCTA were excluded - 73 due to poor image quality not suitable for semi-automated QCT and 208 due to lack of CAD. A total of 260 patients (175 (67%) men, mean age of study population 61 ± 11 years) were included in this study. Demographic data of the 260 included patients are detailed in Table 1. The median (IQR) radiation dose was 3.3 (2.8–4.2) mSv and the mean ± SD Hounsfield attenuation measured in the aorta at the level of the coronary arteries was 515 ± 98 HU. A total of 4420 coronary vessel segments were evaluated for suitability for semi-automated QCT (Fig. 3). In total, 1161 segments with atherosclerotic plaque were quantitatively assessed using fixed and adaptive thresholds.

3.2. Plaque volumes using fixed and adaptive HU thresholds

The two methods used in this study measure the same total plaque volumes but characterizes tissue composition differently. As such, total plaque volumes at lesion level (n = 1161) measured using fixed and adaptive HU thresholds were identical (median (IQR) of 91.7 (47.4, 166.7)). The Bland-Altman analysis showed plaque volumes derived using fixed HU thresholds overestimated NC and DC plaque volumes and underestimated FI and FF plaque volumes compared to plaque volumes derived using adaptive HU thresholds (Fig. 4). Furthermore, these findings became more pronounced with increasing average plaque volumes.

Table 1
Characteristics of the study population (n = 260).

Patient Characteristics	
Age (years), mean ± SD	61 ± 11
Men, n (%)	175 (67)
BMI (kg/m^2), mean ± SD	27.7 ± 4.5
Diabetes, n (%)	33 (13)
Current smoker, n (%)	92 (35)
Former smoker, n (%)	91 (35)
Hypercholesterolemia, n (%)	126 (49)
Hypertension, n (%)	132 (51)
Family history of CAD, n (%)	74 (29)
History of MI, n (%)	44 (17)
Known CAD, n (%)	59 (23)

SD, Standard deviation; BMI, Body Mass Index; CAD, Coronary artery disease; MI, Myocardial infarction.

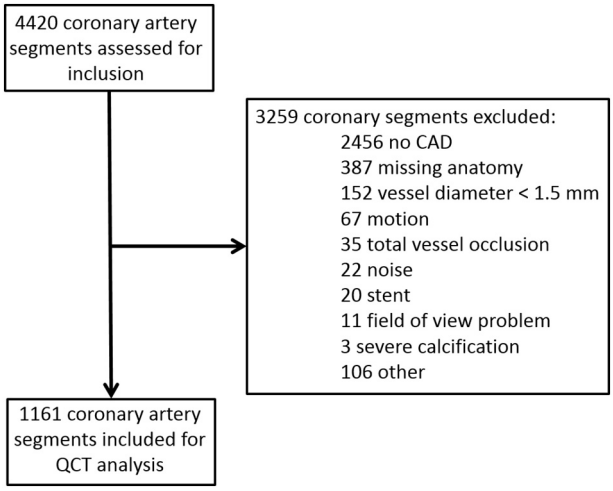

Fig. 3. Flow diagram illustrating the selection process of coronary artery segments for quantitative computer tomography analysis
CAD, Coronary artery disease; QCT, Quantitative computed tomography.

3.3. Plaque volume in lesions stratified by tertiles of HU_{aorta}

Demographic and scan related parameters stratified by tertiles of HU_{aorta} (low (0–467 HU), mid (468–540 HU) and high (541–1024 HU)) are shown in Table 2. No significant differences were found with regards to common cardiovascular risk factors except for age, gender, BMI and body surface area (BSA). Patients with high HU_{aorta} values were predominantly older women with significantly lower BMI and BSA with resultant lower total contrast volumes and kilovoltage compared to patients in the low and mid HU_{aorta} tertiles. Furthermore, no significant differences were found between tertiles with regards to parameters describing coronary plaque distribution and burden. Based on these findings, plaque volumes in low, mid and high HU_{aorta} tertiles were deemed comparable.

When using adaptive HU thresholds, no significant differences in median FI and DC plaque volumes between HU_{aorta} tertiles were found (Fig. 5). Significant differences were, however, found between HU_{aorta} tertiles for FF and NC plaque volumes: median (95% CI) for FF plaque volume in tertile 1 vs tertile 2: 15.74 (13.39;19.67) mm^3 vs 20.63 (17.33;23.30) mm^3, $p < 0.01$; median (95% CI) for NC plaque volume in tertile 1 vs tertile 2: 3.74 (2.26;5.28) mm^3 vs 5.69 (4.90;6.68) mm^3, $p < 0.001$; median (95% CI) for NC plaque volume in tertile 1 vs tertile 3: 3.74 (2.26;5.28) mm^3 vs 5.94 (4.75;7.01) mm^3, $p < 0.001$.

Median plaque volumes of FF, NC and DC measured with fixed HU thresholds differed between HU_{aorta} tertiles. Median FF and NC volumes decreased with increasing HU_{aorta} and DC increased with increasing HU_{aorta}: median (95% CI) for FF plaque volume in tertile 2 vs tertile 3: 19.29 (16.83;21.48) mm^3 vs 15.45 (13.70;16.59) mm^3, $p < 0.01$; median (95% CI) for FF plaque volume in tertile 1 vs tertile 3: 19.10 (16.88;21.52) mm^3 vs 15.45 (13.70; 16.59) mm^3, $p < 0.05$; median (95% CI) for NC plaque volume in tertile 2 vs tertile 3: 9.87 (8.19;11.12) mm^3 vs 8.47 (7.08;9.46) mm^3, $p < 0.05$; median (95% CI) for DC plaque volume in tertile 1 vs tertile 3: 7.73 (5.17;12.31) mm^3 vs 12.02 (8.26;16.24) mm^3, $p < 0.05$. Median FI plaque volume was not significantly different between the low, mid and high HU_{aorta} tertiles.

Median plaque volumes derived using fixed and adaptive HU thresholds are given in Table 3. As demonstrated by the Bland Altman plots in Fig. 4, plaque volumes derived using fixed HU thresholds overestimated DC and NC volumes and underestimated FI and FF volumes compared with plaque volumes derived using adaptive HU thresholds, irrespective of luminal contrast density (Table 3).

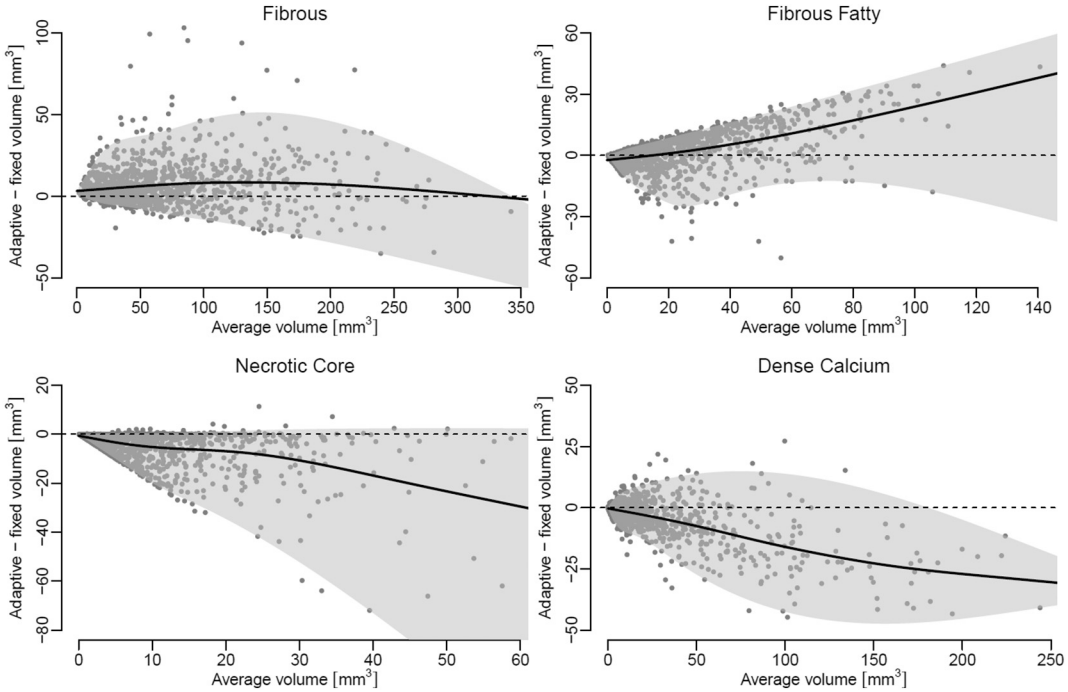

Fig. 4. Bland Altman plots of plaque volumes derived using fixed Hounsfield unit thresholds and adaptive Hounsfield unit thresholds. The solid line represents the mean difference and the shaded area represents the 95% limits of agreement.

4. Discussion

We investigated coronary plaque composition by CCTA in a low-risk unstable angina pectoris population using fixed and adaptive HU thresholds. Firstly, we found that semi-automated quantification of plaque composition using fixed HU thresholds overestimated DC and NC volumes and underestimated FI and FF volumes compared to adaptive HU thresholds. Furthermore, for DC, NC and FF volumes, these over- and underestimations became more pronounced with increasing average plaque volume. Secondly, we found higher attenuation plaque volumes derived using adaptive HU thresholds to be more independent of luminal contrast density compared to fixed HU thresholds. These findings demonstrate the potential feasibility of adaptive HU thresholds for the determination of coronary plaque composition.

Fixed HU thresholds have traditionally been used for the determination of plaque composition. One of the weaknesses of using fixed thresholds to determine plaque composition is the influence of luminal contrast density on the attenuation of the surrounding plaque. Determination of plaque composition may therefore differ from patient to patient as density of the contrast bolus arriving at the heart is influenced by a large number of factors, including body size and cardiac output, that have proven difficult to circumvent [11]. Additionally, comparison of plaque composition between scans performed at different tube voltage may be hampered when using fixed thresholds as luminal contrast density differs with differing tube voltage due to the iodine content of the contrast. Furthermore, the determination of plaque composition may differ within a patient as luminal contrast density falls along the length of a given vessel, is lower in vessel segments with severe stenosis, and may be influenced by blooming artifacts from calcified coronary plaque as calcium blooms significantly more when scanned at lower tube voltage [12,13,24]. Adaptive HU thresholds correct for luminal contrast density and, therefore, potentially measure plaque composition more accurately than when using fixed HU thresholds.

In this study, we found the determination of FI and DC volumes using adaptive thresholds to be independent of luminal contrast density. This finding is supported by the findings of De Graaf et al. who quantitatively analyzed 108 atherosclerotic lesions and compared QCT derived plaque volume measurements with intravascular ultrasound virtual histology (IVUS VH) and found adaptive HU threshold-derived measurements to agree better with IVUS VH than fixed HU threshold-derived measurements [13], as well as the findings by Broersen et al. who found an improved correlation between enhanced IVUS and plaque characterization with adaptive thresholds compared to traditional IVUS [12].

Volumes of NC and FF plaque were not found to be independent of luminal contrast density when using adaptive thresholds. Possible reasons for this may be due to the semi-automated technique used in this study - manual correction may have added to inaccuracies in correctly determining NC plaque which is known to be difficult to identify visually. Numerous studies investigating the reproducibility of quantitatively assessed coronary plaque have found poorer reproducibility of non-calcified and low attenuation plaque compared to other plaque tissue types [7,8] and, as discussed by Papadopoulou et al., variability in the identification of non-calcified plaque could be explained by the incorrect incorporation of the lumen or pericoronary fat in the plaque area [8]. Furthermore, tube voltage does not just affect luminal contrast density but also impacts the measured HU value of all tissues, with higher tube voltage resulting in a lower measured HU value for a given tissue. This may explain the differences in NC and FF plaque volumes with increasing luminal contrast density despite correction. Furthermore, as patients were not their own controls, it cannot be ruled out that there truly were greater plaque volumes of NC in the high HU_{aorta} tertile compared to the low HU_{aorta} tertile. A definitive determination of this would, however, require comparison with a reference standard, which is a limitation of this study.

The potential clinical consequences of employing adaptive thresholds compared to conventional fixed thresholds is important to consider, especially since plaque composition determined using adaptive thresholds compared to using fixed thresholds has been shown to better correlate with IVUS [13]. It has previously been shown that the higher the levels of total non-calcified plaque (NCP) volume a patient has, the higher the risk of adverse cardiac events [3,25]. In this study, we demonstrate that plaque composition derived using fixed HU thresholds

Table 2
Demographic and computed tomography angiography data and tertiles of low, mid and high luminal contrast attenuation in the aorta (HU_{aorta}).

	Low HU_{aorta}	Mid HU_{aorta}	High HU_{aorta}	p-value
Hounsfield units, median (IQR)	442 (405, 455)	509 (483, 522)	595 (565, 659)	–
Heart rate (bpm), mean ± SD	55 ± 10	57 ± 9	57 ± 8	0.44
Contrast (ml), median (IQR)	70 (70, 73)	70 (70, 70)	70 (70, 70)	< 0.01
Kilovoltage				< 0.001
100 kV, n (%)	6 (7)	6 (7)	22 (26)	
120 kV, n (%)	82 (93)	80 (92)	63 (74)	
135 kV, n (%)	0 (0)	1 (0)	0 (0)	
Age, mean ± SD	57 ± 11	60 ± 11	65 ± 10	< 0.0001
Men, n (%)	78 (89)	63 (72)	34 (40)	< 0.0001
BMI (kg/m^2), mean ± SD	28 ± 5	29 ± 4	26 ± 5	< 0.0001
Weight (kg), mean ± SD	89 ± 16	87 ± 13	72 ± 15	< 0.0001
BSA (m^2), mean ± SD	2.07 ± 0.19	2.01 ± 0.16	1.8 ± 0.20	< 0.0001
Diabetes, n (%)	8 (9)	13 (15)	12 (14)	0.45
Current smoker, n (%)	31 (35)	34 (39)	27 (32)	0.60
Hypercholesterolemia, n (%)	38 (43)	46 (53)	42 (49)	0.43
Hypertension, n (%)	43 (49)	47 (54)	42 (49)	0.76
Family history of CAD, n (%)	28 (32)	24 (28)	22 (27)	0.73
History of MI, n (%)	13 (15)	16 (18)	15 (18)	0.80
Known CAD, n (%)	21 (24)	20 (23)	18 (21)	0.91
Vessel disease, n (%)				0.99
Non-obstructive disease (< 50% stenosis)	58 (66)	53 (61)	53 (62)	
1-vessel disease	17 (19)	20 (23)	19 (22)	
2-vessel disease	9 (10)	11 (13)	10 (12)	
3-vessel disease	4 (5)	3 (3)	3 (4)	
Segment involvement score, n (%)[a]				0.66
1–4	47 (53)	40 (46)	37 (44)	
5–8	21 (24)	21 (24)	28 (33)	
9–12	11 (13)	16 (18)	13 (15)	
13–16	9 (10)	10 (12)	7 (8)	
Agatston score, n (%)				0.74
0	10 (11)	9 (10)	7 (8)	
1–10	10 (11)	7 (8)	5 (6)	
11–100	22 (25)	25 (29)	24 (28)	
101–400	25 (28)	18 (21)	26 (31)	
> 400	21 (24)	28 (32)	23 (27)	
Plaque volume in proximal coronary segments, mm3 (median (IQR))[b]	245 (95, 488)	296 (138, 604)	287 (100, 686)	0.43
Total plaque volume in all coronary segments, mm^3 (median (IQR))	301 (106, 620)	322 (146, 771)	328 (114, 806)	0.44

HU, Hounsfield units; SD, standard deviation; IQR, interquartile range; bpm, beats per minute; BMI, body mass index; BSA, body surface area; CAD, coronary artery disease; MI, myocardial infarction.

[a] Segment involvement score defined as 1 point per segment exhibiting coronary plaque, irrespective of degree of stenosis (score 0 to 16).

[b] Proximal coronary segments defined as left main, proximal left anterior descending (LAD), mid LAD, proximal right coronary artery (RCA), mid RCA, and proximal circumflex artery.

overestimated DC and NC volumes and underestimated FI and FF volumes compared to adaptive HU thresholds and that these over- and underestimations became progressively more pronounced with increased average plaque volume. The clinical importance of these findings remains to be investigated in future studies.

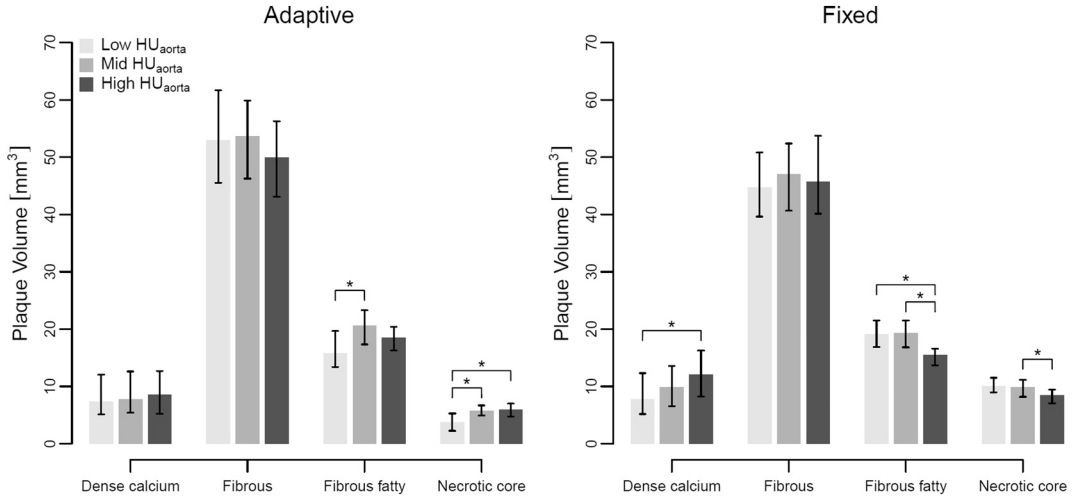

Fig. 5. Plaque volumes measured with adaptive and fixed thresholds, stratified by HU_{aorta}
**Significant p-value.*

Table 3
Dense calcium, fibrous, fibrous fatty and necrotic core plaque volumes derived using adaptive and fixed Hounsfield unit thresholds and stratified by tertile of contrast intensity in the aorta.

HU_{aorta} tertile	Plaque type	Adaptive HU thresholds	Fixed HU thresholds	
		Median (95% CI), mm^3	Median (95% CI), mm^3	P-value
1	Dense calcium	7.34 (5.12;12.03)	7.73 (5.17;12.31)	< 0.05
2	Dense calcium	7.78 (5.40;12.61)	9.83 (6.55;13.57)	< 0.001
3	Dense calcium	8.56 (5.22;12.69)	12.02 (8.26;16.24)	< 0.001
1	Fibrous	52.96 (45.54;61.69)	44.67 (39.65;50.81)	< 0.001
2	Fibrous	53.70 (46.28;59.89)	47.07 (40.66;52.40)	< 0.001
3	Fibrous	49.91 (43.13;56.30)	45.71 (40.14;53.74)	< 0.001
1	Fibrous fatty	15.74 (13.39;19.67)	19.10 (16.88;21.52)	0.135
2	Fibrous fatty	20.63 (17.33;23.30)	19.29 (16.83;21.48)	< 0.001
3	Fibrous fatty	18.51 (16.29;20.41)	15.45 (13.70;16.59)	< 0.001
1	Necrotic core	3.74 (2.26;5.28)	10.01 (8.97;11.51)	< 0.001
2	Necrotic core	5.69 (4.90;6.68)	9.87 (8.19;11.12)	< 0.001
3	Necrotic core	5.94 (4.75;7.01)	8.47 (7.08;9.46)	< 0.001

HU_{aorta}, contrast intensity in the aorta; HU, Hounsfield unit; CI, confidence interval.

4.1. Perspectives

Semi-automated QCT using adaptive HU thresholds could be used in the future to overcome some of the challenges associated with using fixed HU thresholds. Adaptive thresholds, with their potentially more accurate estimation of plaque composition, may give a more correct assessment of plaque vulnerability. Further optimization for the accurate assessment of low attenuation plaques is, however, needed.

4.2. Limitations

This study has some limitations that need to be addressed: Firstly, this study lacks a reference method as confirmation of plaque composition by IVUS was not performed. Studies investigating plaque composition determined by fixed and adaptive HU thresholds and IVUS have, however, previously been performed [13]. Secondly, a study design where each patient is scanned multiple times with different scan protocols would have been optimal for the examination of the effect of luminal contrast density on plaque composition using fixed and adaptive thresholds. This was, however, not possible in the current study design and we deemed patient groups stratified by tertiles of HU_{aorta} to be comparable based on demographic and angiographic likeness with regards to common cardiovascular risk factors and CCTA findings. Thirdly, plaque quantification on CCTA requires high image quality for accurate measurements and is not applicable in small coronary vessels or scans with poor image quality. This may lead to selection bias. Fourthly, the software used for the determination of plaque composition in this study differentiates between four plaque tissue types. It has previously been discussed whether the differentiation of fibrous and lipid tissue is possible as a definitive cut-off for the differentiation of fibrous and lipid tissue has not yet been found [26,27].

5. Conclusions

In conclusion, we found semi-automated quantification of coronary plaque composition using fixed HU thresholds to overestimate DC and NC volumes and underestimate FI and FF volumes compared to adaptive HU thresholds. Furthermore, plaque characterization of higher attenuation plaque volumes using adaptive HU thresholds was more independent of luminal contrast density compared to fixed HU thresholds.

Authorship contributions

MCK and MH made substantial contributions to the conception and design of the work, the acquisition, analysis, interpretation of data, drafting the work and revising it critically for important intellectual content, performed final approval of the version to be published, and agrees to be accountable for all aspects of the work in ensuring that questions related to the accuracy or integrity of any part of the work are appropriately investigated and resolved. AJK, JJL, JTK, JDH, and KFK made substantial contributions to the conception, acquisition, and interpretation of data, revising it critically for important intellectual content, performed final approval of the version to be published, and agrees to be accountable for all aspects of the work in ensuring that questions related to the accuracy or integrity of any part of the work are appropriately investigated and resolved.

Relationship with the industry and financial disclosures

Jesper J Linde has previously received lecturing fees from Toshiba Medical Systems. Martina C de Knegt has previously received lecturing fees from Toshiba Medical Systems and grants from the Danish Heart Foundation and the Danish Agency for Science, Technology and Innovation by The Danish Council for Strategic Research [EDITORS: Eastern Denmark Initiative to improve Revascularization Strategies.

Klaus F Kofoed has received research grants from AP Møller og hustru Chastine McKinney Møllers Fond, The John and Birthe Meyer Foundation, Research Council of Rigshopitalet, The University of Copenhagen, The Danish Heart Foundation, The Lundbeck Foundation, The Danish Agency for Science, Technology and Innovation by The Danish Council for Strategic Research; is principle investigator of the investigator initiated CATCH-2 trial, CSub320 trial and at the steering committee of the CORE320 trial –supported in part by Toshiba Medical Corporation; and is on the Speakers Bureau of Toshiba Medical Systems.

All other authors report no support from any organization for the submitted work; no financial relationships with any organizations that might have an interest in the submitted work in the previous two years; and no other relationships or activities that could appear to have influenced the submitted work.

Funding

This work was supported by the Danish Council for Independent Research (grant number 6110-00443), AP Møller og hustru Chastine McKinney Møllers Fond, The Danish Heart Foundation (grant number 16-R107-A6719-22959) and Eva og Henry Frænkels Mindefond. These funding sources had no role in the study design; in the collection, analysis and interpretation of data; in the writing of the report; and in the decision to submit the article for publication.

References

[1] Versteylen MO, Kietselaer BL, Dagnelie PC, Joosen IA, Dedic A, Raaijmakers RH, et al. Additive value of semiautomated quantification of coronary artery disease using cardiac computed tomographic angiography to predict future acute coronary syndrome. J Am Coll Cardiol 2013;61:2296–305. https://doi.org/10.1016/j.jacc.2013.02.065.

[2] Motoyama S, Sarai M, Narula J, Ozaki Y. Coronary CT angiography and high-risk plaque morphology. Cardiovasc Interv Ther 2013;28:1–8. https://doi.org/10.1007/s12928-012-0140-1.

[3] Kristensen TS, Kofoed KF, Kühl JT, Nielsen WB, Nielsen MB, Kelbæk H. Prognostic implications of nonobstructive coronary plaques in patients with non-ST-segment elevation myocardial infarction: a multidetector computed tomography study. J Am Coll Cardiol 2011;58:502–9. https://doi.org/10.1016/j.jacc.2011.01.058.

[4] Tesche C, Plank F, De Cecco CN, Duguay TM, Albrecht MH, Varga-Szemes A, et al. Prognostic implications of coronary CT angiography-derived quantitative markers for the prediction of major adverse cardiac events. J Cardiovasc Comput Tomogr 2016;10:458–65. https://doi.org/10.1016/j.jcct.2016.08.003.

[5] Deseive S, Straub R, Kupke M, Nadjiri J, Broersen A, Kitslaar PH, et al. Automated quantification of coronary plaque volume from CT angiography improves CV risk prediction at long-term follow-up. JACC Cardiovasc Imaging 2018;11:280–2. https://doi.org/10.1016/j.jcmg.2017.03.010.

[6] Cury RC, Abbara S, Achenbach S, Agatston A, Berman DS, Budoff MJ, et al. CAD-RADS(TM) coronary artery disease - reporting and data system. An expert consensus document of the Society of Cardiovascular Computed Tomography (SCCT), the American College of Radiology (ACR) and the North American Society for Cardiovascular Imaging (NASCI). Endorsed by the American College of Cardiology. J Cardiovasc Comput Tomogr 2016;10:269–81. https://doi.org/10.1016/j.jcct.2016.04.005.

[7] de Knegt MC, Haugen M, Linde JJ, Kühl JT, Nordestgaard BG, Køber LV, et al. Reproducibility of quantitative coronary computed tomography angiography in asymptomatic individuals and patients with acute chest pain. PloS One 2018;13:e0207980https://doi.org/10.1371/journal.pone.0207980.

[8] Papadopoulou S-L, Garcia-Garcia HM, Rossi A, Girasis C, Dharampal AS, Kitslaar PH, et al. Reproducibility of computed tomography angiography data analysis using semiautomated plaque quantification software: implications for the design of longitudinal studies. Int J Cardiovasc Imaging 2013;29:1095–104. https://doi.org/10.1007/s10554-012-0167-5.

[9] Dalager MG, Bøttcher M, Andersen G, Thygesen J, Pedersen EM, Dejbjerg L, et al. Impact of luminal density on plaque classification by CT coronary angiography. Int J Cardiovasc Imaging 2011;27:593–600. https://doi.org/10.1007/s10554-010-9695-z.

[10] Schroeder S, Flohr T, Kopp AF, Meisner C, Kuettner A, Herdeg C, et al. Accuracy of density measurements within plaques located in artificial coronary arteries by X-ray multislice CT: results of a phantom study. J Comput Assist Tomogr 2001;25:900–6.

[11] Bae KT. Intravenous contrast medium administration and scan timing at CT: considerations and approaches. Radiology 2010;256:32–61. https://doi.org/10.1148/radiol.10090908.

[12] Broersen A, de Graaf MA, Eggermont J, Wolterbeek R, Kitslaar PH, Dijkstra J, et al. Enhanced characterization of calcified areas in intravascular ultrasound virtual histology images by quantification of the acoustic shadow: validation against computed tomography coronary angiography. Int J Cardiovasc Imaging 2015. https://doi.org/10.1007/s10554-015-0820-x.

[13] de Graaf MA, Broersen A, Kitslaar PH, Roos CJ, Dijkstra J, Lelieveldt BPF, et al. Automatic quantification and characterization of coronary atherosclerosis with computed tomography coronary angiography: cross-correlation with intravascular ultrasound virtual histology. Int J Cardiovasc Imaging 2013;29:1177–90. https://doi.org/10.1007/s10554-013-0194-x.

[14] Linde JJ, Kofoed KF, Sørgaard M, Kelbæk H, Jensen GB, Nielsen WB, et al. Cardiac computed tomography guided treatment strategy in patients with recent acute-onset chest pain: results from the randomised, controlled trial: CArdiac cT in the treatment of acute CHest pain (CATCH). Int J Cardiol 2013;168:5257–62. https://doi.org/10.1016/j.ijcard.2013.08.020.

[15] Kühl JT, Hove JD, Kristensen TS, Norsk JB, Engstrøm T, Køber L, et al. Coronary CT angiography in clinical triage of patients at high risk of coronary artery disease. Scand Cardiovasc J SCJ 2017;51:28–34. https://doi.org/10.1080/14017431.2016.1207799.

[16] Boogers MJ, Broersen A, van Velzen JE, de Graaf FR, El-Naggar HM, Kitslaar PH, et al. Automated quantification of coronary plaque with computed tomography: comparison with intravascular ultrasound using a dedicated registration algorithm for fusion-based quantification. Eur Heart J 2012;33:1007–16. https://doi.org/10.1093/eurheartj/ehr465.

[17] Yang G, Kitslaar P, Frenay M, Broersen A, Boogers MJ, Bax JJ, et al. Automatic centerline extraction of coronary arteries in coronary computed tomographic angiography. Int J Cardiovasc Imaging 2012;28:921–33. https://doi.org/10.1007/s10554-011-9894-2.

[18] Leipsic J, Abbara S, Achenbach S, Cury R, Earls JP, Mancini GJ, et al. SCCT guidelines for the interpretation and reporting of coronary CT angiography: a report of the Society of Cardiovascular Computed Tomography Guidelines Committee. J Cardiovasc Comput Tomogr 2014;8:342–58. https://doi.org/10.1016/j.jcct.2014.07.003.

[19] Bland JM, Altman DG. Statistical methods for assessing agreement between two methods of clinical measurement. Lancet 1986;1:307–10.

[20] Koenker RW. Quantile Regression (Econometric Society Monographs). Camb Univ Press; 2005. https://doi.org/10.1017/CBO9780511754098. n.d.

[21] Datta S, Satten GA. Rank-sum tests for clustered data. J Am Stat Assoc 2005;100:908–15.

[22] Rosner B, Glynn RJ, M-LT Lee. The Wilcoxon signed rank test for paired comparisons of clustered data. Biometrics 2006;62:185–92. https://doi.org/10.1111/j.1541-0420.2005.00389.x.

[23] R Core Team. R: A language and environment for statistical computing version 3.5.2. Vienna, Austria: R Foundation for Statistical Computing; 2018.

[24] Choi J-H, Min JK, Labounty TM, Lin FY, Mendoza DD, Shin DH, et al. Intracoronary transluminal attenuation gradient in coronary CT angiography for determining coronary artery stenosis. JACC Cardiovasc Imaging 2011;4:1149–57. https://doi.org/10.1016/j.jcmg.2011.09.006.

[25] Nadjiri J, Hausleiter J, Jähnichen C, Will A, Hendrich E, Martinoff S, et al. Incremental prognostic value of quantitative plaque assessment in coronary CT angiography during 5 years of follow up. J Cardiovasc Comput Tomogr 2016;10:97–104. https://doi.org/10.1016/j.jcct.2016.01.007.

[26] Voros S, Rinehart S, Qian Z, Vazquez G, Anderson H, Murrieta L, et al. Prospective validation of standardized, 3-dimensional, quantitative coronary computed tomographic plaque measurements using radiofrequency backscatter intravascular ultrasound as reference standard in intermediate coronary arterial lesions: results from the ATLANTA (assessment of tissue characteristics, lesion morphology, and hemodynamics by angiography with fractional flow reserve, intravascular ultrasound and virtual histology, and noninvasive computed tomography in atherosclerotic plaques) I study. JACC Cardiovasc Interv 2011;4:198–208. https://doi.org/10.1016/j.jcin.2010.10.008.

[27] Pohle K, Achenbach S, Macneill B, Ropers D, Ferencik M, Moselewski F, et al. Characterization of non-calcified coronary atherosclerotic plaque by multi-detector row CT: comparison to IVUS. Atherosclerosis 2007;190:174–80. https://doi.org/10.1016/j.atherosclerosis.2006.01.013.